

Convolutional Neural Networks Trained to Identify Words Provide a Good Account of Visual Form Priming Effects

Dong Yin^a, Valerio Biscione^a, Jeffrey S. Bowers^a

^a*Department of Psychology, University of Bristol, Bristol, BS8 1TL, United Kingdom*

Abstract

A wide variety of orthographic coding schemes and models of visual word identification have been developed to account for masked priming data that provide a measure of orthographic similarity between letter strings. These models tend to include hand-coded orthographic representations with single unit coding for specific forms of knowledge (e.g., units coding for a letter in a given position or a letter sequence). Here we assess how well a range of these coding schemes and models account for the pattern of form priming effects taken from the Form Priming Project and compare these findings to results observed in with 11 standard deep neural network models (DNNs) developed in computer science. We find that deep convolutional networks perform as well or better than the coding schemes and word recognition models, whereas transformer networks did less well. The success of convolutional networks is remarkable as their architectures were not developed to support word recognition (they were designed to perform well on object recognition) and they classify pixel images of words (rather artificial encodings of letter strings). The findings add to the recent work of (Hannagan et al., 2021) suggesting that convolutional networks may capture key aspects of visual word identification.

Keywords: orthographic coding, Deep Neural Networks, human visual system, Form Priming, convolutional DNNs, Vision Transformers

Contents

1	Introduction	3
1.1	Orthographic coding schemes and models of word identification	3
1.2	Deep Neural Network	5
2	Methods	6
2.0.1	Human Priming Data	6
2.0.2	Orthographic coding schemes and word recognition models	6
2.0.3	DNN models	8
2.1	Measuring perceptual similarity of the various DNNs	10
3	Results	12
4	Discussion	16
5	Conflict of Interest Statement	18
6	Declarations	18
6.1	Author Contributions	18
6.2	Data Availability	18
6.3	Code availability	18
6.4	Ethics statement	18
6.5	Consent to Publish	18
6.6	Funding	18
6.7	Consent to Participate	19
Appendix A		
	Similarity Values	24
Appendix B		
	Data Generation	25

1. Introduction

Skilled visual word identification requires extensive experience with written words. It entails identifying the visual characteristics of letters (e.g., oriented lines), mapping these features onto letters, coding for letter order, and eventually selecting word candidates from one’s vocabulary (Carreiras et al., 2014). The process of representing the identity and orders of letters in a letter string is referred to as orthographic coding and constitutes a crucial component of word identification, with different models of word identification adopting different orthographic coding schemes.

Much of the empirical research directed at distinguishing different orthographic coding schemes and models of word identification more generally comes from priming studies that vary the similarity of the prime and target. Various priming procedures have been used, but the most common is the masked Lexical Decision Task (LDT) as introduced by Forster et al. (1987). The procedure involves measuring how quickly people classify a target stimulus as word or nonword when briefly preceded by a prime. The basic finding is that orthographically similar prime strings speed responses to the targets relative to unrelated priming strings (e.g., Schoonbaert and Grainger 2004; Burt and Duncum 2017; Bhide et al. 2014). The assumption is that the greater the priming the greater the orthographic similarity between the prime and the target. A variety of different models of letter coding and models of word identification more broadly have been developed in an attempt to account for more variance in masked form priming experiments.

The primary objective of the current study is to investigate to what extent artificial Deep Neural Network (DNN) models developed in computer science and designed to classify images of objects can account for masked form priming data, and in addition, compare their successes to some standard models of orthographic coding and models of word recognition. In all we test 11 DDNs (different versions of convolutional and transformer networks), five orthographic coding schemes, and three models of visual recognition, as well as two control conditions, as detailed below.

1.1. Orthographic coding schemes and models of word identification

Any model of word recognition needs to include a series of basic processes. This includes encoding the letters and their order, a process of mapping the ordered letters onto lexical representations, and finally a manner of selecting one lexical entry from others. Different models adopt different accounts of

these basic processing. Most relevant for present purposes, models in the psychological literature have taken three basic approaches to encoding letters and letter orders, namely, slot-based coding, context-based coding, and context-independent coding.

On slot-based coding schemes, separate slots of position-specific letter codes are assumed. For example, the word CAT might be coded by activating the three letter codes C_1 , A_2 , and T_3 , whereas the word ACT would be coded as A_1 , C_2 , and T_3 (where the subscript indexes letter position). Because letter codes are conjunctions of letter identities and letter position, the letter A_1 and A_2 are simply different letters (accordingly, CAT and ACT only share one letter, namely T_3).

On context-based coding schemes letters are coded in relation to other letters in the letter string. For example, in open-bigram coding schemes (e.g., Grainger and Whitney 2004), a letter string is coded in terms of all of the ordered letter pairs that it contains. For example CAT is coded by the letter pairs CA, AT, and CT, whereas ACT is coded as AC, AT, and CT. Various different versions of context-based coding schemes (and different versions of open-bigrams) have been proposed, and these again impact on how transposing letters and other manipulations impact on the orthographic similarity between letter strings.

Finally, on context-independent coding schemes, letter units are coded independently of position and context. That is, a node that codes the letter A is activated when the input stimulus contains an A, irrespective of its serial position or surrounding context (the same C, A, and T letter units are part of CAT and ACT). The ordering of letter is computed on-line, and this is achieved in various ways. For example, on the spatial coding scheme (Davis, 2010b), the precise time at which units are activated is used to code letter order. Again, various versions of context-independent coding schemes have been proposed with consequences on the orthographic similarity of letter strings.

These different orthographic coding schemes form the front end of more complete models of visual word identification that include processes that select word representations from these orthographic encodings. For example, the Interactive Activation (IA) Model (McClelland and Rumelhart, 1981), the overlap model (Gomez et al., 2008), and the Bayesian Reader (Norris, 2006) all adopt different versions of slot coding; the open bigram (Grainger et al., 2004) and Seriol (Whitney, 2001) models use different context-based encoding schemes; the spatial coding (Davis, 2010b) and SOLAR models

(Davis, 2001) uses context independent encoding scheme. Note, the predictions of masked priming in these models are the product of both the encoding schemes and the additional processes that support to lexical selection. In addition to these models, the Letters in Time and Retinotopic Space (LTRS; Adelman 2011b) model is agnostic to the encoding scheme and instead makes predictions based on the rate at which different features of the stimulus (that could take different forms) are extracted. We will consider how well various orthographic coding schemes as well as models of word identification account for masked priming results reported in the form priming project (Adelman et al., 2014).

1.2. Deep Neural Network

DNNs are a type of artificial neural network in which the input and output layers are separated by multiple (hidden) layers forming a hierarchical structure. Two of the most common types of DNNs are convolutional neural networks (CNNs) and transformers.

CNNs are inspired by retinotopic organization present in many areas of the primate neo-cortex (Felleman and Van Essen 1991; Krubitzer and Kaas 1993; Sereno et al. 2015): a set of feature detectors (kernels) repeat at different spatial locations to produce a series of feature maps (analogous to simple cells in V1 for example), to which more feature detectors can be applied, hierarchically, to form more and more complex feature detectors.

In contrast, Vision Transformers (ViTs; Dosovitskiy et al. 2020) do not include any convolutions but do introduce attention mechanisms that have been compared to human attention (but see Lindsay 2021 where she points out differences).

CNNs and transformers are highly successful engineering tools that support a wide range of challenging tasks, including visual object recognition. Importantly, CNNs and transformers have been claimed to provide good models of the human visual system, and indeed, are the most successful models in predicting judgments of category typicality (Lake et al., 2015) and predicting object classification errors (Jozwik et al., 2017) on several datasets. CNNs in particular have been good at predicting the neural activation patterns elicited during object recognition in both human and non-human primates' ventral visual processing streams (Cichy et al., 2016; Storrs et al., 2021). A benchmark called Brain-Score has recently been developed to assess similarities between biological visual systems and DNNs (Schrimpf et al., 2018). The best performing models on the Brain-Score benchmarks are

often described as the best models of human vision, and CNNs are currently the best performing models on this benchmark.

More relevant for the present context, Hannagan et al. (2021) demonstrated that training a CNN (CORnet-Z; Kubiľius et al. 2018) to recognize words leads the model to reproduce some key findings regarding visual-orthographic processing in the human visual word form area (VWFA) as observed with fMRI, such as case, font, and word length invariance. In addition, the model’s word recognition ability was mediated by a restricted set of reading-selective units. When these units were removed to simulate a lesion, it caused a reading-specific deficit, similar to the effects produced by lesions to the VWFA.

The current work explores this topic further by determining to what extent CNNs and Transformers account for human orthographic coding as measured through masked form priming effects. Given past reports of DNN-human similarity it might be predicted that DNNs will account for some form priming effects. What is less clear is how well DNNs capture orthographic similarity patterns in comparison to various orthographic coding schemes and models of word identification that were specifically designed to explain form priming effects (amongst other findings). Given that DNNs do not include any hand-built orthographic knowledge and are trained to classify pixel images of words, it would be impressive if these models do as well.

2. Methods

2.0.1. Human Priming Data

Human priming data was sourced from the Form Priming Project (FPP; Adelman et al. 2014) and was used to assess how well various psychological DNN models account for orthographic similarity. FPP contains reaction times for 28 prime types across 420 six-letter word targets gathered from over 924 participants. The prime types and priming effects are shown in Table 1. To measure the priming effect size, the mRT of each prime condition is compared to the mRT of unrelated arbitrary strings (e.g., ‘pljokv’ for the word ‘design’).

2.0.2. Orthographic coding schemes and word recognition models

As discussed above, numerous orthographic coding schemes and word recognition models have been developed to account for orthographic priming effects in humans. Here we assess how well five coding schemes and three

Prime Type	Code Relative to 123456	Relative to ‘DESIGN’	Priming Score
1: Identity	123456	design	42.7
2: Final deletion	12345	desig	34.2
3: Suffix	123456d	designl	33.7
4: Final transposition	123465	desing	32.5
5: Medial transposition	132456/124356/123546	desgin	31.4
6: Medial deletion	13456/12456/12356/12346	dsign	29.6
7: Final substitution	12345d	desigj	29.5
8: Initial substitution	d23456	pesign	29.2
9: Initial transposition	213456	edsign	29.0
10: Central insertion	123d456	desrign	29.0
11: Prefix	d123456	mdesign	26.7
12: Half	123/456	des	25.8
13: Repeated letter	123DD456	deshhign	25.5
14: Central-double-deletion	1256	degn	24.9
15: Medial substitution	1d3456/12d456/123d56/1234d6	desihn	22.7
16: Neighbour once removed	12d356/13d456/124d56/123d46	dsign	21.8
17: 2 apart transposition	143256/125436	degisn	20.2
18: Central double insertion	123dd456	desaxign	19.4
19: All-transposed	214365	edisng	16.8
20: Central double substitution	12dd56	dewvgn	14.9
21: Reversed halves	321654	sedngi	13.4
22: 3-apart-transposition	153426	dgsien	9.9
23: Interleaved halves	415263	idgens	8.9
24: Transposed halves	456123	igndes	8.8
25: Unrelated pseudoword	dddddd	voctal	4.8
26: Reversed except initial	165432	dngise	2.9
27: Central quadruple substitution	1dddd6	dzbtkn	2.3
28: Unrelated arbitrary	dddddd	cbhaux	0

Table 1: The 28 prime types from the FPP. Each prime type denotes the transformation of a given target word into a string via transposing, removing, or adding letters. The numbers in the second column indicated the letters of the prime relative to the target. For example, the prime type ‘final-deletion’ in the second row transforms the word ‘DESIGN’ by deleting the last letter into the string ‘desig’. When multiple codes (e.g., 123/456) are specified, it indicates that each of these sub-conditions contains an equal number of targets. When ‘d’ or ‘D’ is specified, a random letter not found in the target is used. When ‘d’ is specified multiple times, the same letter is not reused. When ‘D’ is specified multiple times, the same letter is reused. Edited from Adelman et al. (2014).

models of word identification account for the priming effects reported in FPP dataset, namely:

1. Orthographic coding schemes
 - (a) Absolute position coding
 - (b) Spatial Coding
 - (c) Binary Open Bigram
 - (d) Overlap Open Bigram
 - (e) SERIOL Open Bigram
2. Full priming models
 - (a) The Interactive Activation Model
 - (b) The Letters in Time and Retinotopic Space Model
 - (c) The Spatial Coding Model

In order to determine the degree of priming we used the match value calculator created by Davis (2010a) that implements the five orthographic coding schemes. For each coding scheme, the calculator takes two strings as input and returns a match value that indicates their predicted similarity. It is assumed that the greater the orthographic similarity, the greater the priming. Note, for any given coding scheme and priming condition, the match value for any target word is the same across target words. For example, in the final deletion condition noted in Table 1, the example target given is DESIGN, but the same exact similarity score is computed for all the targets in this condition (because the prime and target all share the first 5 letters, with only the final letter mismatching; e.g., DESIG and ABDUC).

For the models of visual word identification we assessed orthographic similarity on the basis of their predicted priming scores. IA and SCM implementations were taken from Davis (2010b) and LTRS model was taken from a simulator developed by Adelman (2011a). For each model the mean reaction time (mRT) were computed for each related prime condition and compared with the mRT in the unrelated arbitrary condition.

2.0.3. DNN models

We trained seven common convolutional networks (CNNs) and four Vision Transformer networks (ViTs). The convolutional models belong to the families of AlexNet (Krizhevsky et al., 2012), VGG (Simonyan and Zisserman, 2014), ResNet (He et al., 2016), DenseNet (Huang et al., 2016) and EfficientNet (Tan and Le, 2019), and all Transformers were from the ViTs

family (Dosovitskiy et al., 2020). We included transformer models as they are one of the most common architectures currently use in the machine learning literature and there are claims that these models do a better job in capturing human vision in some conditions (Tuli et al., 2021). All models were pretrained on ImageNet (Deng et al., 2009) to initialise the weights. The ViTs listed in Table 2 vary in their complexities and a number of properties including number of layers and attention heads.

After pretraining, the final classifier layer was removed and the models were trained to classify images of 1000 different words (the same number used by Hannagan et al. 2021), with each word represented as a one-hot encoded vector. All 420 six letter words from From Priming Project were used and the remaining 580 were sourced from Google’s Trillion Word Corpus (Google, 2011). The lengths of the 580 words were evenly distributed between three, four, five, seven, and eight letters, with 116 words chosen at each length. As with the Form Priming Project’s 420 words, the 580 words are chosen to not contain the same letter twice to ensure conditions like the transposed letter primes (e.g., 213456) are not identical to the original string. The complete list is available through the GitHub repository of the current study (Yin, 2022).

	Family	Model	Accuracy(%)
	AlexNet	AlexNet	99.3
	DenseNet	DenseNet169	99.8
	EfficientNet	EfficientNet-B1	99.9
Convolution	ResNet	ResNet50	100
		ResNet101	99.9
	VGG	VGG16	99.7
		VGG19	99.8
Transformer	ViT	ViT-B/16	98.2
		ViT-B/32	100
		ViT-L/16	99.9
		ViT-L/32	99.8

Table 2: DNN Models’ performance on the word recognition task using the validation dataset. Accuracy denotes the probability that a model’s prediction (the one with the highest probability) matches the correct response.

We employed data augmentation techniques to diversify the visual representation of each word by manipulating font, size, rotation of letters, and

by changing the position of the image in space, referred to as translation (See Figure 1 for some examples; for details of augmentation see Figure B.5). We generated 6,000 images for each word, resulting in a dataset containing 6,000,000 images. 5,000,000 images are used for training, while the remaining 1,000,000 are used for performance validation. The algorithm for generating datasets is described in detail in Appendix B. For training the Adam optimizer and the cross-entropy loss function are used. A hyperparameter search is performed for the learning rate using a random grid-search, yielding a value of 1e-5. When the training average loss stops improving by a specified threshold of 0.0025, the training was terminated. The accuracy of the models on the validation set of words is reported in Table 2.

We then generated a dataset of prime words. To generate this dataset, each of the 420 Form Priming Project words was transformed into 28 prime types. For example, the target word ‘ABDUCT’ was transformed into ‘baduct’ for the ‘initial transposition’ condition, ‘abdutc’ for the ‘final transposition’ condition, and so forth. Each prime is used to generate an image using the Arial font, resulting in 11,760 images (420 target words \times 28 prime types). No rotation or translation variations at the letter level are introduced, and all strings are positioned at the centre of the image using the same font size of 26, which is the average size used for training.

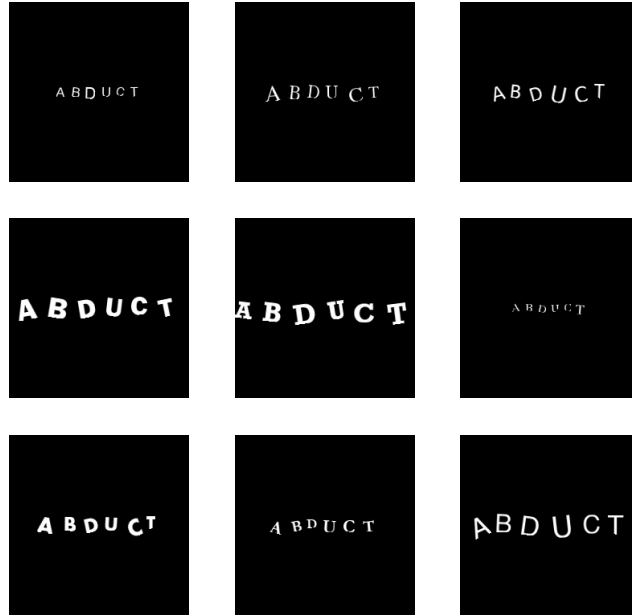
2.1. Measuring perceptual similarity of the various DNNs

To measure the the perceptual similarity between two stimulus images in a model we compared the unit activations at the penultimate layer when each of the stimuli is presented as an input to the network using Cosine Similarity (CS):

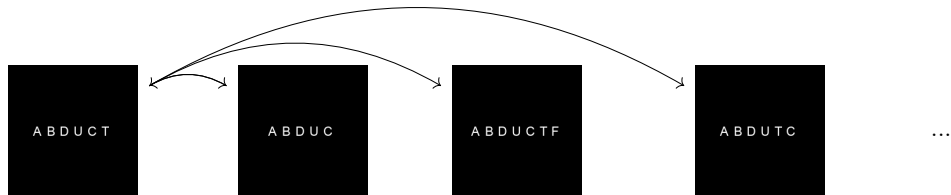
$$CS(A, B) := \frac{A \cdot B}{\|A\| \|B\|} \quad (1)$$

CS ranges from -1 (opposite internal representation) to 1 (identical internal representation).

We examine the mean values of cosine similarity for each condition for each model. The correlation (τ) between the priming demonstrated by the 28 priming scores by humans and the mean cosine similarities found in model M is then computed (that is, each value of cosine similarity is computed by averaging across test images for a word). We then create a new vector $PX \times$ by sampling 28 values from the vector PX with replacement (i.e., some of the pairings (p_i, x_i) will repeat, while others will be absent). This is repeated a



(a) Training Data



Target Stimulus Prime: Final Deletion Prime: Suffix Prime: Final Transposition ...

(b) Priming Data

Figure 1: Image examples of **(a)**: training data; **(b)**: priming data using the word ABDUCT.

thousand times, yielding vectors $PX \times (1), \dots, PX \times (1000)$. Using Kendall's correlation coefficient, we obtain the correlation coefficients, $\tau \times (1)$ through $\tau \times (1000)$. Finally, we compute the variance of our 1000 samples to determine the standard error of τ .

We also included three baseline conditions to better understand the priming effects observed. First, the *CS* between the pixels of prime and target images was computed. For this calculation each pixel is considered a distinct dimension, and the angle between the vectors of the two word images is cal-

culated. This served as a baseline for determining the extent to which the models contribute to orthographic similarity scores beyond the pixel values between stimuli. In addition we used ImageNet pretrained models (without any training on letter strings) and ImageNet pretrained models fine-tuned on 1000 classes of six-letter random strings as two additional baselines. This was done to assess the role of training DNNs on English words on the pattern of form priming effects obtained. Using the aforementioned method, the mean values of cosine similarity for each model condition are calculated, and the average correlation coefficient was used for each model class. Due to the use of the mean values, these metrics do not have error bars on Figure 2. Note, only the results of the control model pretrained on ImageNet are presented in Figure 2 – the results of control model fine-tuned on random letter strings were very similar.

3. Results

Figure 2 plots Kendall’s correlation, over the 28 prime types, between the human priming data the various orthographic coding schemes (as measured by match values), models of word identification (as measured by predicted priming scores), DNNs (as measured by cosine similarity scores), as well as various baseline measures of similarity. See Figure B.6 for matrix that plots the full set of correlations.

The most striking finding is that the CNNs did a good job in predicting the pattern of human priming scores across conditions, with correlations ranging from $\tau = .49$ (AlexNet) to $\tau = .71$. (ResNet101) with all p-values $< .01$. Indeed, the CNNs performed similarly to the various orthographic coding schemes word recognition models, and often better. This contrasts with the relatively poor performance of the Transformer networks, with τ ranging from .25 to .38.

Importantly, the good performance of the CNNs was not due to the pixel value similarity between the prime-target images as the pixel control condition (pixCS) has no significant correlation with the human priming data. It is also not simply the product of the architectures of the CNNs as the predictions were much poorer for the CNNs pretrained on ImageNet but not trained on English words. Rather, it is the combination of the CNN architectures with training on English words that led to good performance.

A more detailed assessment of the overlap between DNNs, orthographic coding schemes and word identification models is provided in Figures 3 and

4 that depict the distribution of responses in each condition for all models as well as summarize the priming results per condition. From this, it is clear that all the CNNs had particular difficulty in predicting the priming in ‘half’ condition (as indicated by the red arrow) in which either first three letters or the final three letters served as primes (The CNNs substantially underestimated the priming in this condition). A similar difficulty was found in many of the psychological models as well, but the effect was not quite so striking. There were no other prime conditions that led to such a large and consistent error in any model or coding scheme.

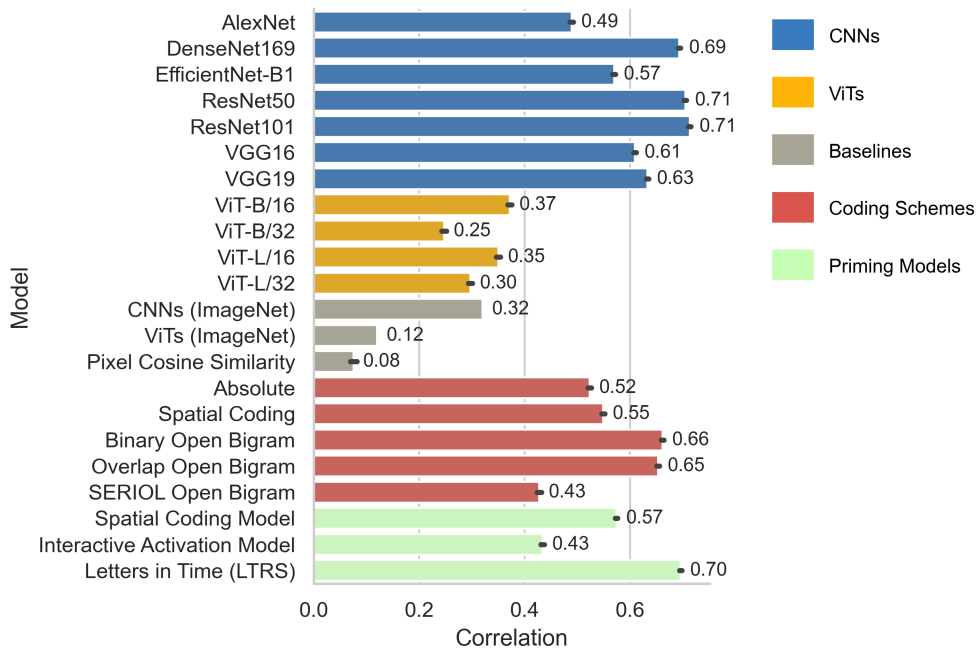


Figure 2: Priming (correlation) scores between model predictions and human data for each DNN, coding scheme, priming model, and baseline. The term “LTRS” refers to the Letters in Time and Retinotopic Space. The error bars represent the standard errors of the correlation distribution for each model.

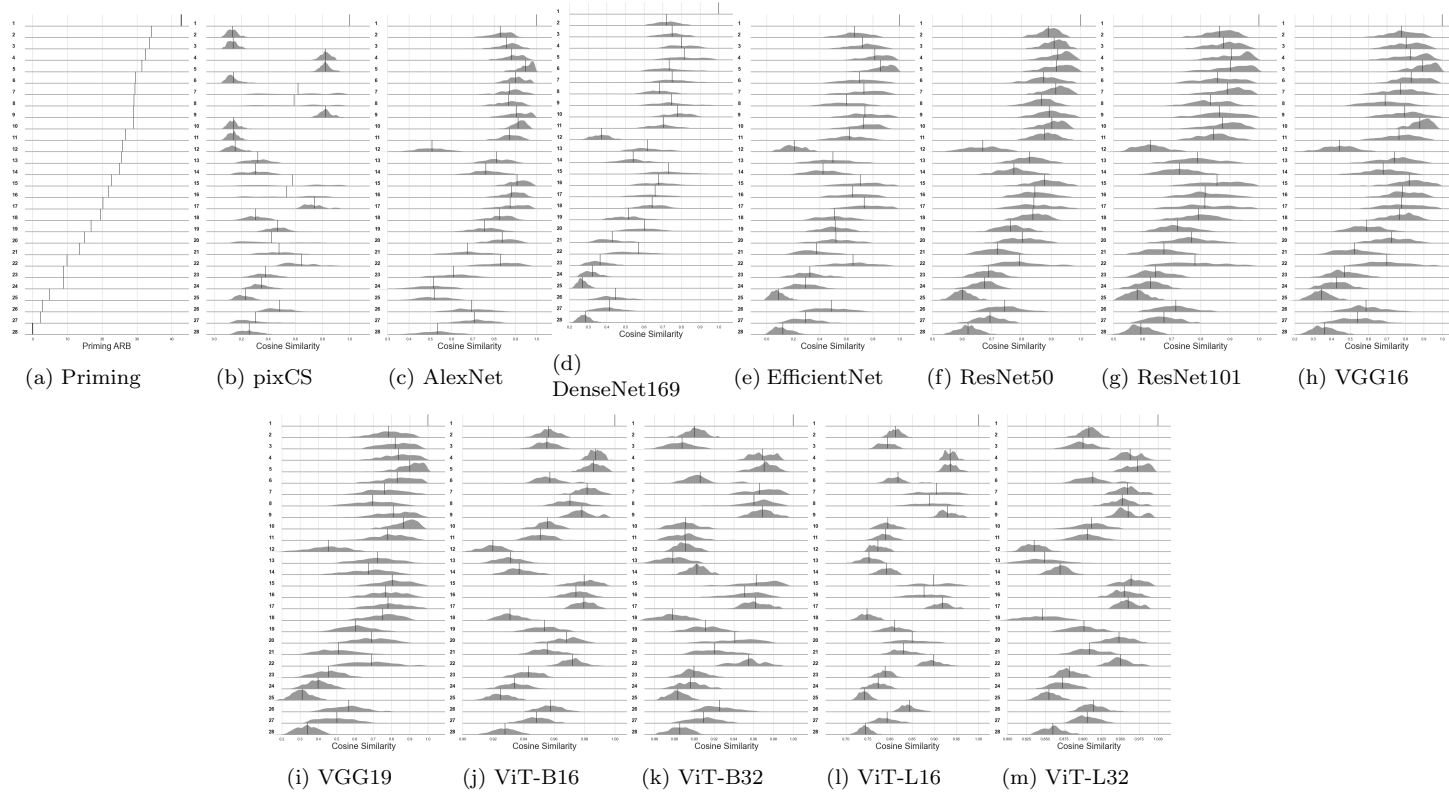


Figure 3: Distributions of Human Priming and the DNN Models Perception. For each subplot, the x-axis is the metric specific similarity measure similarity (W, T_j) and the y-axis is the prime conditions T . Priming scores, calculated as $mRT_{\text{unrelated arbitrary string condition}} - mRT_{\text{prime type}}$. Prime types are ordered according to the size of priming effect in the human data (largest to smallest), as in Table 1. As illustrated in the first row, the ‘identity’ condition has the strongest priming effect as it has the highest priming score of 42.69ms. Priming score for a condition is the difference of its mRT and the ‘unrelated arbitrary’ condition. See table 1 for the index of the 28 conditions.

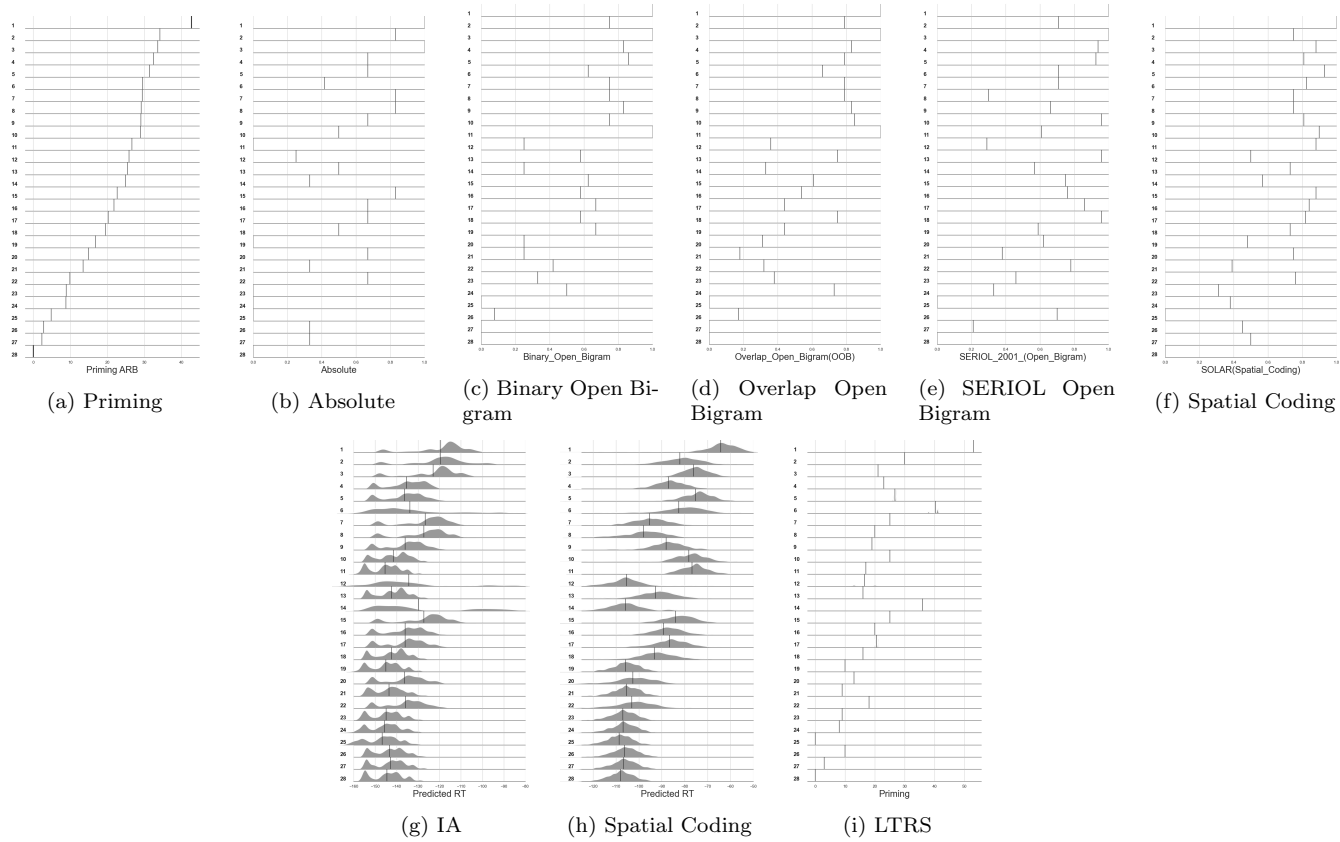


Figure 4: Distributions of Human Priming and the coding schemes. For each subplot, the x-axis is the metric specific similarity measure similarity (W, T_j) and the y-axis is the prime conditions T . See table 1 for the index of the 28 conditions. The Interactive Activation and Spatial Coding Model values are made negative to obtain a positive correlation coefficient with human priming data, as they represent estimated RTs that is negatively correlated with priming effect size.

4. Discussion

A wide number of orthographic coding schemes and models of visual word identification have been designed to account for masked form priming effects that provide a measure of the orthographic similarities between letter strings. Here we assessed how well these standard approaches account for the form priming effects reported in the Form Priming Project (Adelman et al., 2014) and compared to the results to two different classes of DNNs (CNNs and Transformers). Strikingly, the CNNs we tested did similarly, and in some cases better, than the psychological models specifically designed to explain form priming effects. This is despite the fact that the CNN architectures were designed to perform well in object identification rather than word identification, and despite the fact that the models were trained to classify pixel images of words rather than hand-built and artificial encoding of letter strings.

By contrast, we found that visual transformers are less successful in accounting for form priming effects in humans, suggesting that these models are identifying images of words in a non-human like way. In some ways this is surprising given past findings that the pattern of errors observed in object recognition is more similar between visual transformers and humans compared to CNNs and humans (Tuli et al., 2021). But at the same time, our findings are consistent with the finding that CNNs provide the best predictions of neural activation in the ventral visual stream during object recognition as measured by Brain-Score (Schrimpf et al., 2018) and other brain benchmarks. Indeed, visual transformers (similar to the ones we tested here) do much worse on Brain-Score compared to CNNs, with the top performing transformer model performing outside the top-100 models on the current Brain-Score leader-board. To the extent that better performance on Brain-Score reflects a greater similarity between DNNs and humans, our finding that CNNs do a better job than transformers in accounting for masked form priming makes sense.

Our findings are also consistent with recent work by Hannagan et al. who found that a CNN trained to classify images of words and objects show a number of hallmark findings of human visual word recognition. This includes CNNs learning units that are both selective for words (analogous to neurons in the visual word form area) as well as invariant to letter size, font or case. Furthermore, lesioning these units led to selective difficulties in identifying words (analogous to dyslexia following lesions to the visual word form area).

Interestingly, the authors also provided evidence that the CNN learned a complex combination of position specific letter codes as well as bigram representations. It seems that these learned representations are also able to account for a substantial amount of of form priming effects observed in humans. The observation that CNNs not only account for a range of empirical phenomena regarding human visual word identification, but in addition, perform well on various brain benchmarks for visual object identification lends some support to the "recycling hypothesis" according to which a subpart of the ventral visual pathway initially involved in face and object recognition visual is repurposed for letter recognition (Hannagan et al., 2021).

Despite these successes, it is important to note that there is a growing number of studies highlighting that CNNs fail to capture most key low-level, mid-vision, and high-level vision findings reported in psychology (Bowers et al., in press). Indeed, most CNNs that perform well on brain-score do not even classify objects on the basis of shape, and rather, classify objects on the basis of texture (Geirhos et al., 2018). And when models are trained to have a shape bias when classifying objects they have a non-human shape bias (Malhotra et al., in press).

How is it possible to obtain such high good performance brain benchmarks such as Brain-Score and account for few findings from psychology? Bowers et al. (also see Dujmović et al. 2021) argued that the good performance on these benchmarks may provide a misleading estimate of CNN-human similarity with good performance reflecting two very different systems picking up on different sources of information that are correlated with each other. For instance it is possible that texture representations in CNNs are used not only to identify objects but also are used to predict the neural activation of ventral visual system that identifies objects based on shape. Indeed, Dujmović et al. 2021 have run simulations showing that CNNs that are designed to recognize objects in a very different way nevertheless can support good predictions of brain activations based on confounds that are common in image datasets.

In some ways this makes the current findings all the most impressive, as the CNNs are doing well at accounting for a complex set of priming conditions that were specifically designed to contrast different hypotheses regarding orthographic coding schemes. Of course, there were some notable failures of the CNNs accounting for form priming (most notably all the CNNs underestimated the amount of priming in the half condition in which the primes were composed of the first three or final three letters of the target), and there may be many additional priming conditions that may prove problematic for

CNNs. Nevertheless, the current results do highlight that CNNs should be given more attention in psychology as models of human visual word recognition.

5. Conflict of Interest Statement

The authors declare that the research was conducted in the absence of any commercial or financial relationships that could be construed as a potential conflict of interest.

6. Declarations

6.1. Author Contributions

J.S.B and V.B were responsible for the design and supervision of the study. D.Y specified the statistical approach and wrote the scripts for data generation and analyses. All authors contributed to the analysis of the data and interpretation and writing of the paper.

6.2. Data Availability

The code that generate the data that support the findings of this study are available at: <https://github.com/Don-Yin/Orthographic-DNN>

6.3. Code availability

The code that support the findings of this study are available at: <https://github.com/Don-Yin/Orthographic-DNN>

6.4. Ethics statement

The present study was approved by the School of Psychological Science Research Ethics Committee.

6.5. Consent to Publish

We certify that the paper contains no personal information (names, initials, or any other information which could identify an individual person) that would infringe upon that person's right to privacy.

6.6. Funding

This project has received funding from the European Research Council (ERC) under the European Union's Horizon 2020 research and innovation programme (grant agreement No 741134).

6.7. Consent to Participate

Not Applicable.

References

- Adelman, J. (2011a). Letters in Time and Retinotopic Space.
- Adelman, J. S. (2011b). Letters in time and retinotopic space. *Psychological Review*, 118(4):570–582.
- Adelman, J. S., Johnson, R. L., McCormick, S. F., McKague, M., Kinoshita, S., Bowers, J. S., Perry, J. R., Lupker, S. J., Forster, K. I., Cortese, M. J., Scaltritti, M., Aschenbrenner, A. J., Coane, J. H., White, L., Yap, M. J., Davis, C., Kim, J., and Davis, C. J. (2014). A behavioral database for masked form priming. *Behavior Research Methods*, 46(4):1052–1067.
- Bhide, A., Schlaggar, B. L., and Barnes, K. A. (2014). Developmental differences in masked form priming are not driven by vocabulary growth. *Frontiers in Psychology*, 5.
- Bowers, J. S., Malhotra, G., Dujmović, M., Montero, M. L., Tsvetkov, C., Biscione, V., Puebla, G., Adolfs, F. G., Hummel, J., Heaton, R. F., Evans, B. D., Mitchell, J., and Blything, R. (in press 2022). Deep Problems with Neural Network Models of Human Vision. *PsyArXiv*.
- Burt, J. S. and Duncum, S. (2017). Masked form Priming is Moderated by the Size of the Letter-Order-Free Orthographic Neighbourhood. *Quarterly Journal of Experimental Psychology*, 70(1):127–141.
- Carreiras, M., Armstrong, B. C., Perea, M., and Frost, R. (2014). The what, when, where, and how of visual word recognition. *Trends in Cognitive Sciences*, 18(2):90–98.
- Cichy, R. M., Khosla, A., Pantazis, D., Torralba, A., and Oliva, A. (2016). Comparison of deep neural networks to spatio-temporal cortical dynamics of human visual object recognition reveals hierarchical correspondence. *Scientific Reports*, 6(1).
- Davis, C. (2001). The self-organising lexical acquisition and recognition (SO-LAR) model of visual word recognition. *The Sciences and Engineering*.
- Davis, C. (2010a). The Spatial Coding Model (Colin J. Davis 2010).
- Davis, C. J. (2010b). The spatial coding model of visual word identification. *Psychological Review*, 117(3):713–758.

- Deng, J., Dong, W., Socher, R., Li, L.-J., Li, K., and Fei-Fei, L. (2009). Imagenet: A large-scale hierarchical image database. In *2009 IEEE conference on computer vision and pattern recognition*, pages 248–255. Ieee.
- Dosovitskiy, A., Beyer, L., Kolesnikov, A., Weissenborn, D., Zhai, X., Unterthiner, T., Dehghani, M., Minderer, M., Heigold, G., Gelly, S., Uszkoreit, J., and Houlsby, N. (2020). An Image is Worth 16x16 Words: Transformers for Image Recognition at Scale. *arXiv*.
- Dujmović, M., Hummel, J., and Bowers, J. (2021). Human shape representations are not an emergent property of learning to classify objects. *bioRxiv*.
- Felleman, D. J. and Van Essen, D. C. (1991). Distributed Hierarchical Processing in the Primate Cerebral Cortex. *Cerebral Cortex*, 1(1):1–47.
- Forster, K. I., Davis, C., Schoknecht, C., and Carter, R. (1987). Masked priming with graphemically related forms: Repetition or partial activation? *The Quarterly Journal of Experimental Psychology Section A*, 39(2):211–251.
- Geirhos, R., Rubisch, P., Michaelis, C., Bethge, M., Wichmann, F., and Brendel, W. (2018). ImageNet-trained CNNs are biased towards texture; increasing shape bias improves accuracy and robustness. *arXiv*.
- Gomez, P., Ratcliff, R., and Perea, M. (2008). The overlap model: A model of letter position coding. *Psychological Review*, 115(3):577–600.
- Google (2011). Google Books Ngram Viewer – Google Product.
- Grainger, J., Heuven, V., and Walter, J. B. (2004). Modeling Letter Position Coding in Printed Word Perception. *Nova Science Publishers*.
- Grainger, J. and Whitney, C. (2004). Does the huamn mnid raed wrods as a wlohe? *Trends in Cognitive Sciences*, 8(2):58–59.
- Hannagan, T., Agrawal, A., Cohen, L., and Dehaene, S. (2021). Simulating the emergence of the Visual Word Form Area: Recycling a convolutional neural network for reading. *The Proceedings of the National Academy of Sciences (PNAS)*.

- He, K., Zhang, X., Ren, S., and Sun, J. (2016). Deep Residual Learning for Image Recognition. *2016 IEEE Conference on Computer Vision and Pattern Recognition (CVPR)*.
- Huang, G., Liu, Z., Maaten, L., and Weinberger, K. (2016). Densely Connected Convolutional Networks. *arXiv*.
- Jozwik, K. M., Kriegeskorte, N., Storrs, K. R., and Mur, M. (2017). Deep Convolutional Neural Networks Outperform Feature-Based But Not Categorical Models in Explaining Object Similarity Judgments. *Frontiers in Psychology*, 8.
- Krizhevsky, A., Sutskever, I., and Hinton, G. E. (2012). ImageNet classification with deep convolutional neural networks. *Communications of the ACM*, 60(6):84–90.
- Krubitzer, L. A. and Kaas, J. H. (1993). The dorsomedial visual area of owl monkeys: Connections, myeloarchitecture, and homologies in other primates. *The Journal of Comparative Neurology*, 334(4):497–528.
- Kubilius, J., Schrimpf, M., Nayebi, A., Bear, D., Yamins, D. L. K., and DiCarlo, J. J. (2018). CORnet: Modeling the Neural Mechanisms of Core Object Recognition. *bioRxiv*.
- Lake, B., Zaremba, W., Fergus, R., and Gureckis, T. (2015). Deep Neural Networks Predict Category Typicality Ratings for Images. *Cognitive Science Society*.
- Lindsay, G. W. (2021). Convolutional Neural Networks as a Model of the Visual System: Past, Present, and Future. *Journal of Cognitive Neuroscience*, 33(10):2017–2031.
- Malhotra, G., Dujmović, M., Hummel, J., and Bowers, J. (in press 2021). The contrasting shape representations that support object recognition in humans and cnns.
- McClelland, J. L. and Rumelhart, D. E. (1981). An interactive activation model of context effects in letter perception: I. An account of basic findings. *Psychological Review*, 88(5):375–407.

- Norris, D. (2006). The Bayesian reader: Explaining word recognition as an optimal Bayesian decision process. *Psychological Review*, 113(2):327–357.
- Schoonbaert, S. and Grainger, J. (2004). Letter position coding in printed word perception: Effects of repeated and transposed letters. *Language and Cognitive Processes*, 19(3):333–367.
- Schrimpf, M., Kubilius, J., Hong, H., Majaj, N. J., Rajalingham, R., Issa, E. B., Kar, K., Bashivan, P., Prescott-Roy, J., Geiger, F., Schmidt, K., Yamins, D. L. K., and DiCarlo, J. J. (2018). Brain-Score: Which Artificial Neural Network for Object Recognition is most Brain-Like? *Brain-Score: Which Artificial Neural Network for Object Recognition is most Brain-Like?*
- Sereno, M. I., McDonald, C. T., and Allman, J. M. (2015). Retinotopic organization of extrastriate cortex in the owl monkey—dorsal and lateral areas. *Visual Neuroscience*, 32.
- Simonyan, K. and Zisserman, A. (2014). Very Deep Convolutional Networks for Large-Scale Image Recognition. *arXiv*.
- Storrs, K. R., Kietzmann, T. C., Walther, A., Mehrer, J., and Kriegeskorte, N. (2021). Diverse Deep Neural Networks All Predict Human Inferior Temporal Cortex Well, After Training and Fitting. *Journal of Cognitive Neuroscience*, pages 1–21.
- Tan, M. and Le, Q. V. (2019). EfficientNet: Rethinking Model Scaling for Convolutional Neural Networks. *arXiv*.
- Tuli, S., Dasgupta, I., Grant, E., and Griffiths, T. (2021). Are Convolutional Neural Networks or Transformers more like human vision? *arXiv*.
- Whitney, C. (2001). How the brain encodes the order of letters in a printed word: The SERIOL model and selective literature review. *Psychonomic Bulletin and Review*, 8(2):221–243.
- Yin, D. (2022). Orthographic DNNs.

Appendix A. Similarity Values

Prime Type	Priming-ARB	CNNs							ViTs			
		AlexNet	DenseNet169	Efficientnet-B1	ResNet50	ResNet101	VGG16	VGG19	ViT-B/16	ViT-B/32	ViT-L/16	ViT-L/32
ID	42.69	1.00	1.00	1.00	1.00	1.00	1.00	1.00	1.00	1.00	1.00	1.00
DL-1F	34.23	0.83	0.72	0.66	0.89	0.87	0.78	0.78	0.96	0.90	0.81	0.91
IL-1F	33.66	0.86	0.75	0.72	0.91	0.88	0.80	0.82	0.96	0.89	0.79	0.90
TL56	32.46	0.88	0.80	0.82	0.92	0.91	0.83	0.84	0.99	0.97	0.94	0.96
TL-M	31.42	0.95	0.81	0.86	0.92	0.90	0.89	0.90	0.99	0.97	0.94	0.97
DL-1M	29.56	0.90	0.73	0.70	0.88	0.86	0.83	0.83	0.96	0.91	0.82	0.91
SN-F	29.45	0.87	0.75	0.73	0.92	0.89	0.77	0.76	0.98	0.97	0.91	0.96
SN-I	29.16	0.87	0.68	0.60	0.87	0.83	0.69	0.70	0.97	0.96	0.89	0.95
TL12	29.03	0.91	0.75	0.74	0.89	0.86	0.79	0.81	0.98	0.97	0.93	0.96
IL-1M	29.00	0.91	0.78	0.73	0.90	0.88	0.88	0.87	0.96	0.89	0.80	0.91
IL-1I	26.67	0.87	0.70	0.62	0.88	0.84	0.77	0.78	0.95	0.89	0.79	0.91
SUB3	25.83	0.51	0.37	0.21	0.67	0.63	0.44	0.45	0.92	0.89	0.77	0.84
IL-2MR	25.48	0.81	0.62	0.50	0.83	0.79	0.74	0.72	0.93	0.88	0.75	0.85
DL-2M	24.91	0.76	0.54	0.42	0.77	0.73	0.68	0.67	0.94	0.90	0.79	0.87
SN-M	22.68	0.91	0.73	0.70	0.88	0.86	0.82	0.80	0.98	0.96	0.90	0.96
N1R	21.77	0.88	0.68	0.65	0.85	0.82	0.78	0.77	0.97	0.95	0.88	0.95
NATL-24/35	20.20	0.88	0.66	0.73	0.84	0.81	0.78	0.78	0.98	0.96	0.92	0.96
IL-2M	19.42	0.82	0.64	0.51	0.84	0.79	0.77	0.75	0.93	0.88	0.75	0.85
T-All	16.77	0.75	0.52	0.52	0.76	0.72	0.59	0.60	0.95	0.91	0.81	0.90
DSN-M	14.94	0.84	0.60	0.52	0.80	0.77	0.72	0.69	0.97	0.94	0.85	0.95
RH	13.44	0.68	0.43	0.38	0.72	0.67	0.52	0.51	0.96	0.92	0.83	0.91
NATL25	9.91	0.83	0.57	0.65	0.79	0.78	0.70	0.69	0.97	0.96	0.90	0.95
IH	8.90	0.61	0.36	0.33	0.69	0.64	0.47	0.46	0.94	0.90	0.79	0.88
TH	8.80	0.51	0.32	0.29	0.68	0.63	0.43	0.40	0.93	0.90	0.77	0.87
ALD-PW	4.80	0.52	0.27	0.09	0.60	0.58	0.35	0.31	0.92	0.88	0.74	0.86
RF	2.86	0.69	0.45	0.49	0.74	0.71	0.59	0.57	0.96	0.93	0.84	0.91
EL	2.34	0.71	0.42	0.29	0.69	0.67	0.54	0.50	0.95	0.91	0.79	0.91
ALD-ARB	0.00	0.53	0.28	0.12	0.62	0.59	0.36	0.34	0.93	0.89	0.74	0.86

Table A.3: Priming-ARB: index of priming size (ms); CNNs, ViTs: mean cosine similarity.

Prime Type	Coding Schemes					Priming Models			Baseline
	Absolute	SC	BOB	OOB	SOB	SCM	IA	LTRS	PixCS
ID	1.00	1.00	1.00	1.00	1.00	-63.00	-119.00	53.00	1.00
DL-1F	0.83	0.75	0.75	0.79	0.71	-82.00	-117.00	30.00	0.14
IL-1F	1.00	0.88	1.00	1.00	1.00	-76.00	-121.00	21.00	0.14
TL56	0.67	0.81	0.83	0.83	0.94	-87.00	-133.00	23.00	0.82
TL-M	0.67	0.93	0.86	0.79	0.93	-75.00	-133.00	26.67	0.82
DL-1M	0.42	0.83	0.63	0.66	0.71	-82.00	-130.00	40.25	0.14
SN-F	0.83	0.75	0.75	0.79	0.71	-95.00	-124.00	25.00	0.62
SN-I	0.83	0.75	0.75	0.79	0.30	-98.00	-124.00	20.00	0.59
TL12	0.67	0.81	0.83	0.83	0.66	-88.00	-133.00	19.00	0.82
IL-1M	0.50	0.90	0.75	0.85	0.96	-78.00	-139.00	25.00	0.14
IL-II	0.00	0.88	1.00	1.00	0.61	-76.00	-143.00	17.00	0.14
SUB3	0.25	0.50	0.25	0.36	0.29	-105.00	-130.00	16.50	0.16
IL-2MR	0.50	0.73	0.58	0.75	0.96	-93.00	-140.00	16.00	0.32
DL-2M	0.33	0.57	0.25	0.33	0.57	-106.00	-125.00	36.00	0.31
SN-M	0.83	0.88	0.63	0.61	0.75	-84.00	-124.00	25.00	0.58
N1R	0.67	0.84	0.58	0.54	0.76	-89.00	-133.00	20.00	0.53
NATL-24/35	0.67	0.82	0.67	0.44	0.86	-86.00	-133.00	20.50	0.74
IL-2M	0.50	0.73	0.58	0.75	0.96	-93.00	-140.00	16.00	0.31
T-All	0.00	0.48	0.67	0.44	0.59	-106.00	-143.00	10.00	0.47
DSN-M	0.67	0.75	0.25	0.31	0.62	-103.00	-133.00	13.00	0.42
RH	0.33	0.39	0.25	0.18	0.38	-105.00	-141.00	9.00	0.48
NATL25	0.67	0.76	0.42	0.32	0.78	-103.00	-133.00	18.00	0.65
IH	0.00	0.31	0.33	0.38	0.46	-107.00	-142.00	9.00	0.38
TH	0.00	0.38	0.50	0.73	0.33	-107.00	-143.00	8.00	0.35
ALD-PW	0.00	0.00	0.00	0.00	0.00	-109.00	-144.00	0.00	0.23
RF	0.33	0.45	0.08	0.17	0.70	-106.00	-141.00	10.00	0.48
EL	0.33	0.50	0.00	0.00	0.21	-107.00	-140.00	3.00	0.31
ALD-ARB	0.00	0.00	0.00	0.00	0.00	-108.00	-142.00	0.00	0.26

Table A.4: Coding schemes, LTRS: predicted match value; SCM and IA: predicted mean reaction time (ms). In order to obtain a positive correlation value, the SCM and IA values are made negative.

Appendix B. Data Generation

Figure B.5 illustrates how the 1,000 target words are used to generate 6,000 images per word algorithmically, which involves the following steps:

1. Apply one of the ten common fonts (e.g., Arial). The complete list can be found at Yin (2022).

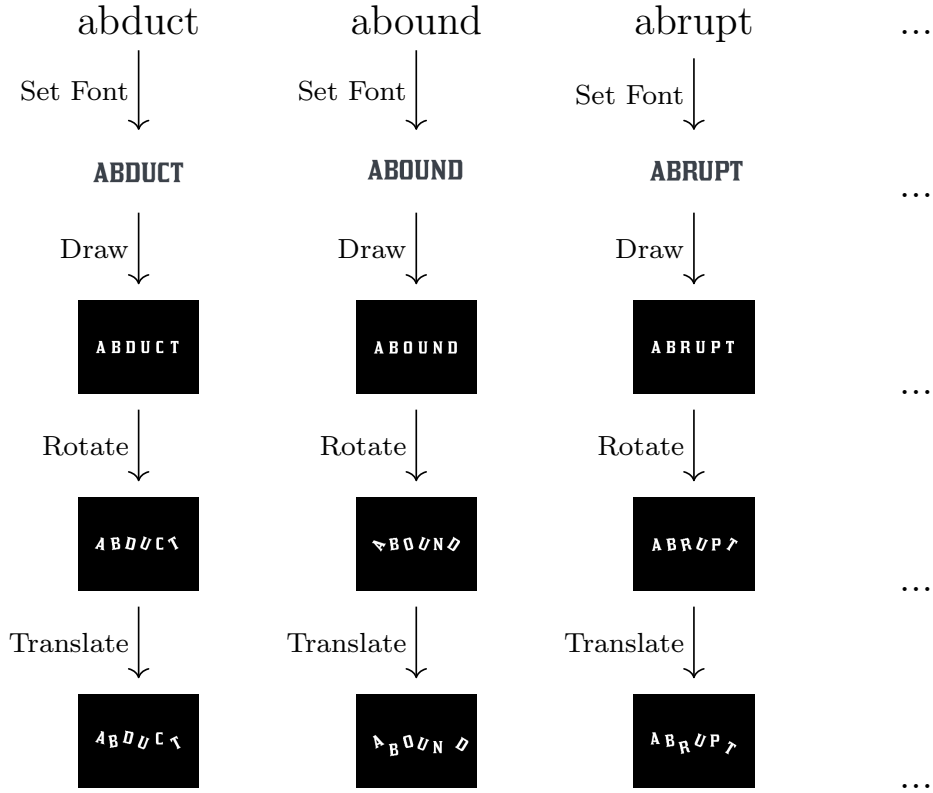


Figure B.5: Illustration of the process of generating training/validation images from target words (e.g., ‘ABDUCT’). The word is drawn with a random font and size. Each letter is then rotated and translated randomly. This procedure is applied on each target word to generate 6,000 images, resulting in 6,000,000 images (1,000 words \times 6,000 images).

2. Apply one of ten sizes selected from $\{x \in 2Z : 18 \leq x < 38\}$
3. Draw the target word as an image.
4. Add random rotation to individual letters using an angle determined by the normal distribution $N(0, \frac{2\pi}{45})$.
5. Add random translation to individual letters so that the updated letter coordinates (x, y) meet the condition shown in Equation B.1, where (a, b) are the letter’s initial coordinates.
6. Transform the image into grayscale.
7. Resize image to 224×224 pixels.

$$\left(0.8 \times \sqrt{\text{height}_{\text{letter}}^2 + \text{width}_{\text{letter}}^2}\right)^2 \geq (x - b)^2 + (y - a)^2 \quad (\text{B.1})$$

$$\forall (a, b) \in \text{Bounding Circle}$$

These operations ensure sufficient variation between the generated images to simulate human perceptual invariance to rotation and spacing. At the end of this process, 6,000,000 images are generated (1,000 words \times 6,000 images). 5,000,000 images are used for training and the remaining 1,000,000 are used for validating the DNN models’ performance.

Architecture	Family	Model	Neural Benchmarks				Behavioural Benchmark	Brain-Score
			V1	V2	V4	IT		
Convolutional	AlexNet	AlexNet	0.51	0.35	0.44	0.36	0.37	0.41
	DenseNet	Densenet169	0.49	0.32	0.5	0.38	0.54	0.45
	EfficientNet	EfficientNet-B1	0.49	0.33	0.49	0.38	0.55	0.45
	ResNet	ResNet50	0.51	0.32	0.49	0.41	0.53	0.45
		ResNet101	0.49	0.34	0.49	0.4	0.56	0.46
	VGG	VGG16	0.43	0.51	0.34	0.48	0.37	0.43
		VGG19	0.54	0.34	0.47	0.36	0.49	0.44
Transformer	ViT	ViT-B/16	0.12	0.26	0.12	0.08	0.34	0.18
		ViT-B/32	0.14	0.29	0.13	0.09	0.28	0.18
		ViT-L/16	0.11	0.27	0.12	0.10	0.33	0.19
		ViT-L/32	0.15	0.30	0.13	0.09	0.29	0.19

Table B.5: The DNNs models and their Brain-Scores (Schrimpf et al., 2018). Each neural benchmark corresponds to a specific area of the visual system. The mean value of benchmarks is calculated to represent an overall ‘Brain-Score’.

Figure B.6 illustrates the pair-wise Kendall’s correlation matrix between the human priming-ARB and the DNN models and baseline similarity metrics (similarity values are listed in Appendix A).

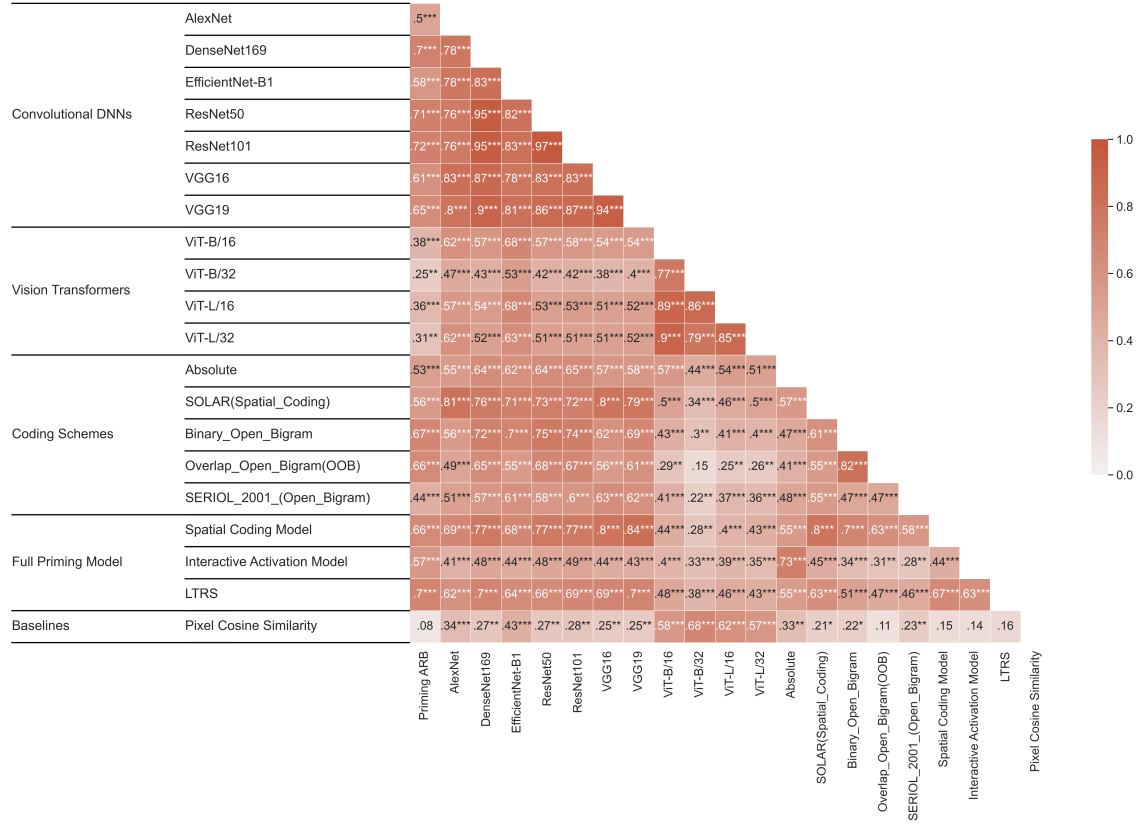


Figure B.6: Pairwise Correlation Matrix Between Human Priming Data, the DNN Models and Other Similarity Metrics. The values represent Kendall's τ correlation coefficients. Priming-ARB is the human priming size using the arbitrary unrelated prime condition as the baseline; pixCS is the Pixel cosine similarity; SCM is the Spatial Coding Model. It should be noted that, in order to obtain a positive correlation value, the LDist and SCM's values are made negative.

* $p < .05$. ** $p < .01$. *** $p < .001$